

*Please select category below:*

Normal Paper

Student Paper

Young Engineer Paper

# Frictional heating as an estimator of modal damping and structural degradation: a vibrothermographic approach

Xintian Chi <sup>1</sup>, Dario Di Maio <sup>2,3</sup>, Nicholas Lieven <sup>1</sup>

<sup>1</sup> *Department of Aerospace Engineering, University of Bristol, Queens Building, University Walk, Bristol, BS8 1TR, England, UK*

<sup>2</sup> *University of Twente, Faculty of Engineering Technology, Horst Complex N138, P.O. Box 217, 7500 AE Enschede, The Netherlands*

<sup>3</sup> *Department of Mechanical Engineering, University of Bristol, Queens Building, University Walk, Bristol, BS8 1TR, England, UK*

## Abstract

This research presents a novel vibrothermographic approach for estimating changes in modal damping and health conditions of vibrating structures using measured temperature increases caused by frictional heat generation. In this article, the theoretical background supporting this method is firstly presented. A metal frame structure connected by bolted joints, which possessed moderate damping that could be manually adjusted by altering the bolt torque in the joints representing different tightness levels and structural health conditions, was studied experimentally so that the changes of dynamic behaviours and the structural degradation could be investigated. Through modal analyses and vibrothermographic tests with six different bolt load levels, the robustness of this method was demonstrated. In the concluding sections of the article, the significance of the observations made in this research is summarised, and the potential of this approach for further development is discussed.

**Keywords:** Structural health monitoring, vibration, vibrothermography, bolted joint, damping, modal analysis, structural dynamics, infrared thermography

## Introduction

With the increasing complexity of modern engineering structures, a wide variety of damage mechanisms that were previously relatively uncommon can now be frequently encountered, making issues in such structures more difficult to detect and causing the structures more prone to failure.

Conventionally, techniques such as vibration testing and modal analysis have been extensively utilised for damage detection and structural health monitoring. As the creation of damage, defects or other issues often causes changes in the dynamics of structures, tracking the dynamic properties, such as natural frequencies, mode shapes and damping ratios, of inspected structures is usually able to reveal the underlying structural degradation [1–5].

However, in reality, such dynamic parameters are not always easily measurable. In many industrial applications, performing vibration tests may require the structures or machines to shut down, which would interrupt their normal operating routine. Because of this requirement, non-contact non-destructive testing (NDT) techniques are becoming increasingly more popular in

relevant fields. Through the application of such methods, the conditions of the structures can be evaluated without causing unnecessary downtime.

In this paper, a novel approach of utilising infrared thermography, which is a typical example of non-contact NDT methods, is presented to reveal both the changes in dynamic properties (modal damping to be more specific) caused by structural degradation and the changes in the health conditions of the structures directly through the measurement of temperature increases caused by frictional heating. Specifically, the practice of applying thermal measurement in vibration tests to evaluate the conditions of structures is commonly referred to as vibrothermography [6–10].

Infrared thermography as a damage detection and structural health monitoring technique possesses several distinct advantages, especially in terms of being able to perform rapid continuous scans of large areas within short measurement times. The results from infrared thermographic tests are usually presented in the form of whole-field two-dimensional images or videos, which are easier to understand compared to most other NDT methods and hence able to lower the difficulty in the subsequent data analysis procedures. These advantages make infrared thermography practically viable for the detection of damage and monitoring of health in large-scale engineering structures due to its high effectiveness and efficiency.

Vibrothermography is a special application of infrared thermography that utilises the vibrations of inspected objects as heat sources. When an object is subjected to vibratory excitation, heat will be generated through the induced vibration. The heat generated inside can subsequently be conducted to the surfaces of the object and detected by an infrared camera, which can then be applied to identify and locate the damage, defects or other issues where the heat is generated. As an application of infrared thermography, vibrothermography also shares the advantages mentioned above. Because of the unique heat generation mechanisms, vibrothermography is particularly useful for detecting certain types of problems such as cracks and delamination [10]. Besides damage detection and structural health monitoring, the thermal data measured in vibrothermographic tests can also be applied to reflect the changes in dynamic properties of the structures, as the latter would fundamentally determine the vibrations of the structures which subsequently affects the heat generation during the vibrations [11, 12].

During this research, a metal frame structure connected by bolted joints, as shown in Fig. 1, was selected as the specimen for the experimental demonstration of this vibrothermographic approach. To elaborate, one of the main reasons leading to the complexity of modern engineering structures is the number of components and the process in which the components are assembled. Through the assembly of the components, joints are created. Among the wide variety of configurations of joints, bolted joints have been extensively studied in research activities due to their varying dynamic properties under different loading and contact conditions [11–19]. A particular concern with bolted joints is that the vibrations of the structures can gradually loosen the joints, threatening the structural integrity and making the already complex dynamics more unpredictable.

At the beginning of the main body of the paper, the theories supporting this proposed vibrothermographic method is explained, where the underlying relationship between frictional heating, damping and the health condition of the vibrating structure is discussed.

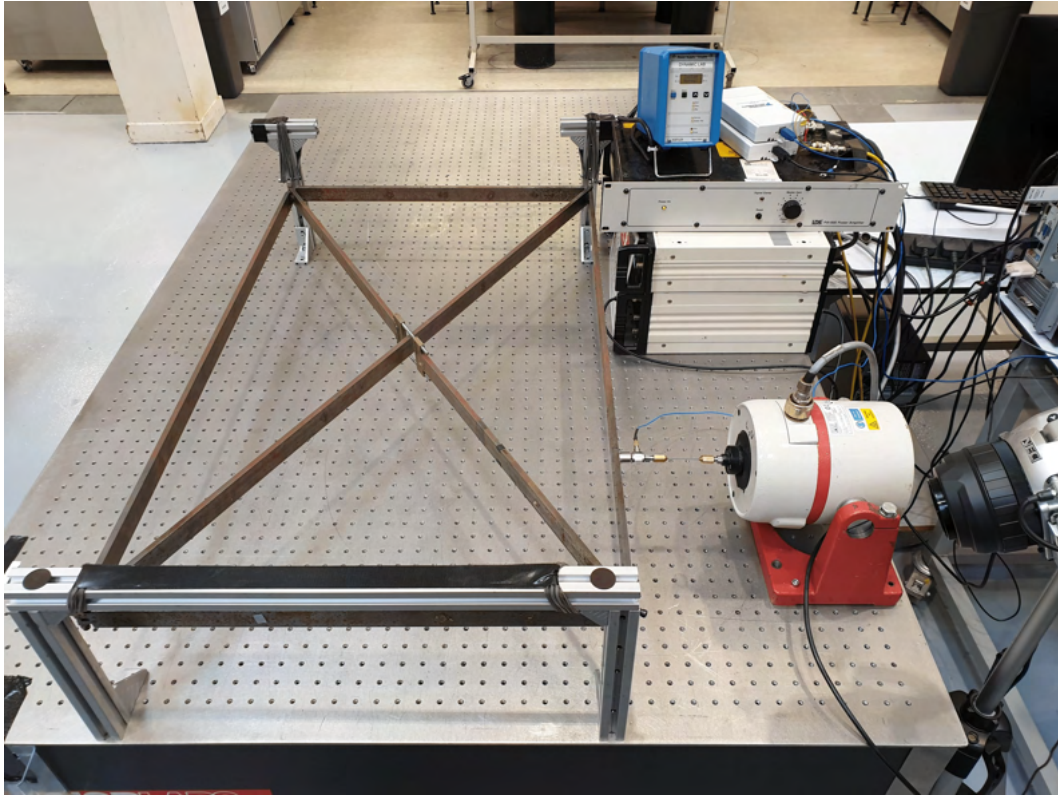


*Fig. 1: The metal frame structure studied in this research*

In the experimental tests of this research, the bolt torque in the joints could be adjusted to simulate different health conditions of the structure. In this process, the dynamic properties of the structure were also altered accordingly. Using the vibration data obtained with a scanning laser Doppler vibrometer (SLDV) and thermal data acquired with an infrared camera, it was shown that both the damping of the structure and the temperature increases in the joints were clearly correlated with the varying bolt torque simulating different conditions of the structure. Based on this observation, it was demonstrated that this vibrothermographic approach was able to rely on the temperature measurement to reveal the underlying changes in the dynamic properties and the health conditions of the structure.

## **Theoretical Background**

As introduced above, vibrothermography, which is a special application of infrared thermography, was applied as the experimental method in this research. Unlike conventional infrared thermographic methods where external heat is applied to the test objects, in vibrothermography heat is generated internally due to the vibrations of the structures through several different mechanisms, including frictional heating, viscoelastic heating, plasticity-induced heat generation and sometimes thermoelastic effect [10, 20].

However, regardless of the exact heat generation mechanism, in order to increase the heat generation for improved thermal contrast, the regions of interest need to possess high strain energy during the induced vibration [7, 9, 20–39]. For this reason, the parameters of the excitation force in vibrothermographic tests, including both the frequency and the location of excitation, should be properly selected to manipulate the deflection shape of the structure so that damage detectability could be enhanced.

For vibrating structures, high strain energy is achieved at or around resonances, so the estimation of strain energy distribution in the test structure could be achieved through modal analysis. In operating conditions, the deflection shape of the test structure is a superposition of all excited mode shapes so calculating the strain energy distribution in each individual mode of vibration through a modal analysis can give predictions on the actual strain energy distribution in the structure. The results from the modal analysis would then be utilised as the guidelines for the subsequent vibrothermographic tests, where the parameters of the excitation could be adjusted to enable sufficient strain energy and hence heat generation in the regions of interest.

For the metal frame structure studied in this research, frictional heating was the most dominant source of heat generation. In this case, the test structure should be excited by mechanical forces or acoustic/ultrasonic waves at a single frequency—or multiple frequencies—so that the relevant regions could produce friction due to the relative motion between surfaces during the induced vibration. Specifically, the area of interest in this research was the contact surfaces in the joints.

The relative motion between the contact surfaces is usually relatively complicated and can be described as a stick-slip process [40–43]. However, only the slip part of the motion would contribute to the frictional heating. For this reason, the stick portion that could not provide frictional heat generation would not be concerned in this research, even though minor heat may still be generated in this process through some of the other mechanisms described above.

Mathematically, when relative motion is present, the local frictional heat generation rate between two contact surfaces during the slip motion can be calculated from:

$$P = F_f \dot{\gamma}, \quad (1)$$

where  $F_f$  is the frictional force which equals the normal force  $F_n$  multiplied by the kinetic friction coefficient  $\mu_k$  while  $\dot{\gamma}$  is the slip rate which is the speed of the relative motion between the contact surfaces [10]. In this metal frame structure, the changes in the contact conditions in the joints caused by the altered bolt load could affect the frictional heat generation by influencing both of the parameters above.

To elaborate, as the bolt load decreased which simulated the loosening of the joint, the contact load between the surfaces would decrease while the slip rate would increase. Although another factor that is the loss of contact between the surfaces could also affect the frictional heat generation, it was verified that it would not make critical differences in this research because of the deflection shape of the metal frame structure. For this reason, it may be predicted that, during the vibrothermographic tests, if all other parameters such as the amplitude and the frequency of vibration remained approximately unchanged, a maximum frictional heat generation rate would exist, which should correspond to a specific contact load level. In this case, as the bolt load in the joint decreased, the frictional heat generation was expected to increase first, and then decrease as the load approached zero so that a bell-curve-shaped relationship should be observed [12].

For the relationship between the bolt load and the dynamic properties of the structure, as the bolt load was reduced, the overall stiffness of the structure should be expected to decrease accordingly, which would cause the decrease of the natural frequencies. Should the influence of the changes be significant, the mode shapes may be altered as well. As for the damping which describes the energy dissipation during the vibrations, because the most dominant source of

energy dissipation was frictional heating in this case, the relationship between the bolt load and the damping ratios should also be able to be approximated as a bell curve.

## Experimental Testing

In order to verify the predictions made above and demonstrate the robustness of this vibrothermographic approach, experimental tests were conducted on the metal frame structure shown in Fig. 1. As mentioned previously, the experimental testing would be started with the modal analysis to obtain the relevant dynamic and modal properties of the structure. The results from the modal analysis could then be utilised to guide the subsequent vibrothermographic tests.

### Rig Set-up for Experimental Testing

The metal frame structure studied in this research was made of mild steel. The overall dimensions of the frame were 1000 mm × 600 mm × 30 mm and the total mass was 10.3 kg. The structure was suspended throughout the experimental tests to minimise the influence of unexpected external factors. As shown in Fig. 1, the structure consisted of six individual beams, which formed four identical and relatively complex joints in the four corners. To demonstrate the connections more clearly, the geometry of the joints is shown in Fig. 2.

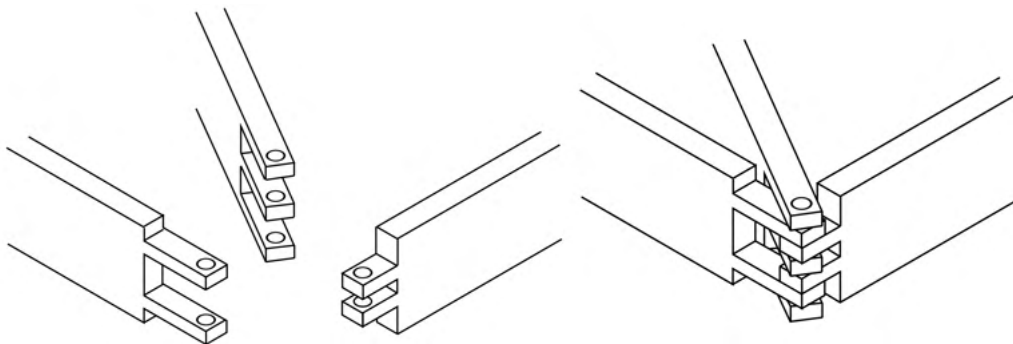


*Fig. 2: The geometry of the joints in the metal frame structure [44]*

To introduce the external excitation in both the modal testing and the vibrothermographic tests, an LDS V406 permanent magnet shaker was attached to the structure via a drive rod, which would be controlled using signals generated on a computer with a LabVIEW panel and amplified through an LDS PA 100E power amplifier. An SLDV system was employed to acquire the vibration data during the modal tests while an infrared camera was applied to measure the temperature changes in the vibrothermographic tests.

### Preliminary Experimental Modal Testing

As explained previously, a modal analysis should be completed first to obtain the modal parameters, including the natural frequencies, mode shapes and strain energy distributions in the structure during its vibration, so the parameters for the vibrothermographic tests could be more properly selected.

As only one joint in the metal frame structure would be inspected during the subsequent vibrothermographic tests, the bolt load in this joint was set to 6 N m using a digital torque wrench, which was approximately the maximum load that could be practically applied, while the bolt loads in the other three joints were lowered to zero. However, for the sake of

completeness, non-zero normal forces still existed in the other three joints due to the mass of the structure supported by the joints, which was inevitable in a practical environment.

Before the experimental tests, a preliminary finite element (FE) analysis was completed on a model created using the physical properties and measured dimensions of the metal frame structure to predict its relevant modal parameters. Based on the results from the FE modal analysis, it was decided to set the frequency range of interest to 10 Hz to 100 Hz in the experimental tests. During the experimental tests, with this frequency range, 10 modes of vibration were successfully discovered. The natural frequencies of the 10 modes are summarised in Table 1 while the mode shapes are presented in Fig. 3.

*Table 1: Natural frequencies of the first 10 modes of vibration of the metal frame structure measured experimentally*

Mode	1	2	3	4	5	6	7	8	9	10
Freq. (Hz)	11.05	17.63	21.86	27.32	54.15	57.42	60.13	62.44	77.56	97.48

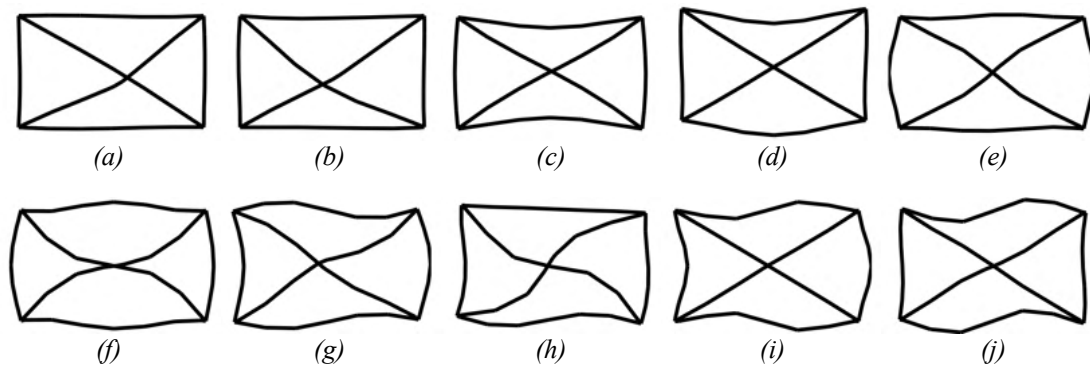


*Fig. 3: Mode shapes of the (a) –(j) first to 10<sup>th</sup> modes of vibration of the metal frame structure measured experimentally [44]*

### **Modal Analysis on the Updated FE Model**

Following the completion of the initial experimental modal tests, the preliminary FE model was updated according to the experimental results. The updated FE model would be utilised to generate the high-resolution mode shapes and strain energy distributions that were unable to be obtained through the experimental tests.

After the completion of the model update, the outputs from the FE modal analysis became almost identical to the experimental results. To present the FE results, the mode shapes of the first 10 modes are displayed in Fig. 4

By comparing the mode shapes in Figs. 3 and 4, it could be observed that nine out of the 10 modes could be correlated. The fifth mode from the FE analysis was an out-of-plane mode, so it was unable to be excited in the experimental tests using an in-plane excitation force, which explained its absence from the experimental results. Besides this mode, all other mode pairs were correlated as their mode shapes appeared to be almost identical. The natural frequencies calculated from the FE analysis were then compared with their experimental counterparts, as summarised in Table 2, showing that the FE model was created and updated correctly so high fidelity could be ensured.



Table 2: Natural frequencies of the first 10 modes of vibration of the metal frame structure, experimental results vs FE outputs

Mode	1	2	3	4	5	6	7	8	9	10
Freq. Exp. (Hz)	11.05	17.63	21.86	27.32	N/A	54.15	57.42	60.13	62.44	77.56
Freq. FE (Hz)	11.26	17.11	20.72	26.57	32.74	54.20	57.63	60.41	62.96	77.96
Diff. (%)	1.90	-2.95	-5.22	-2.75	N/A	0.09	0.37	0.47	0.83	0.52

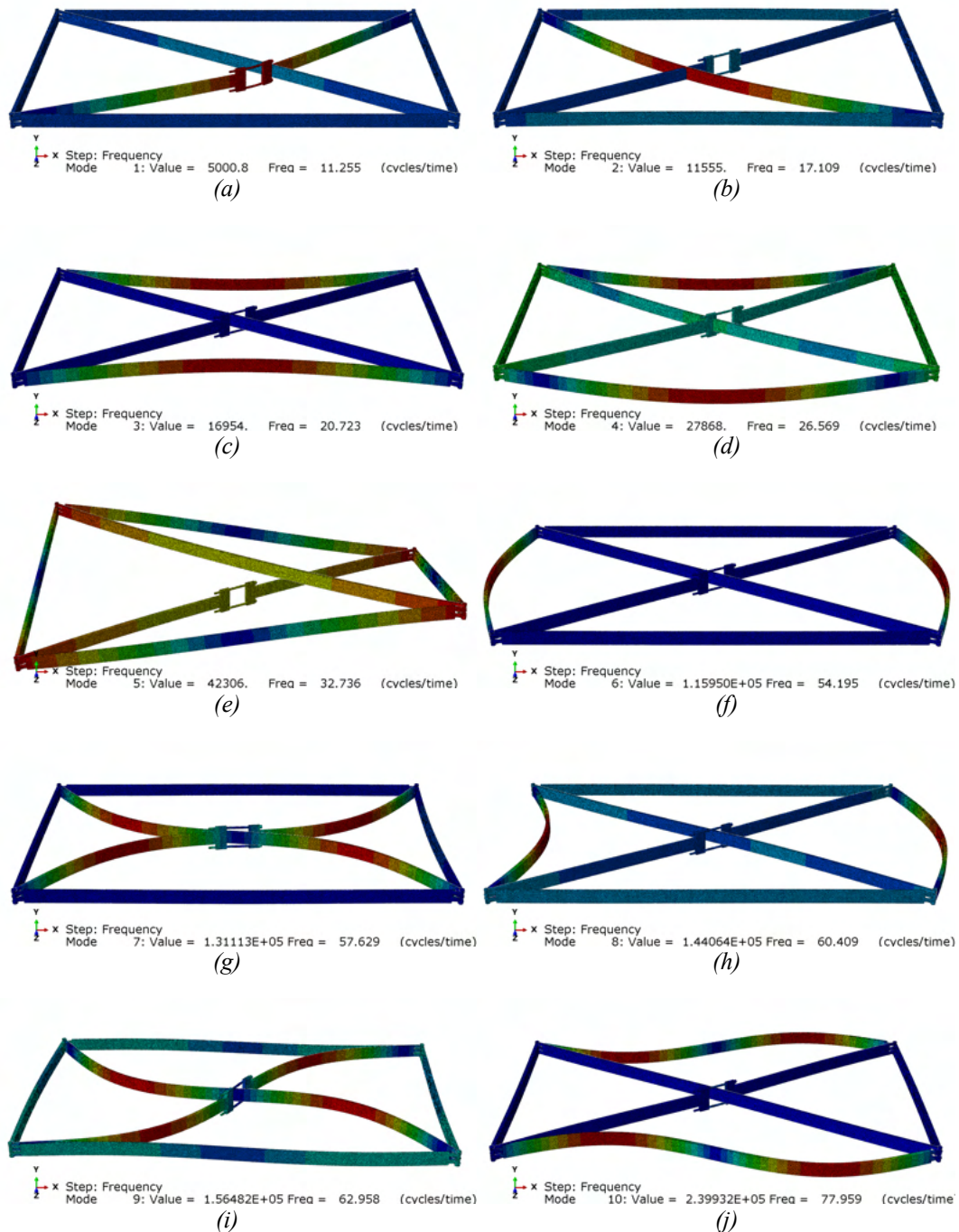
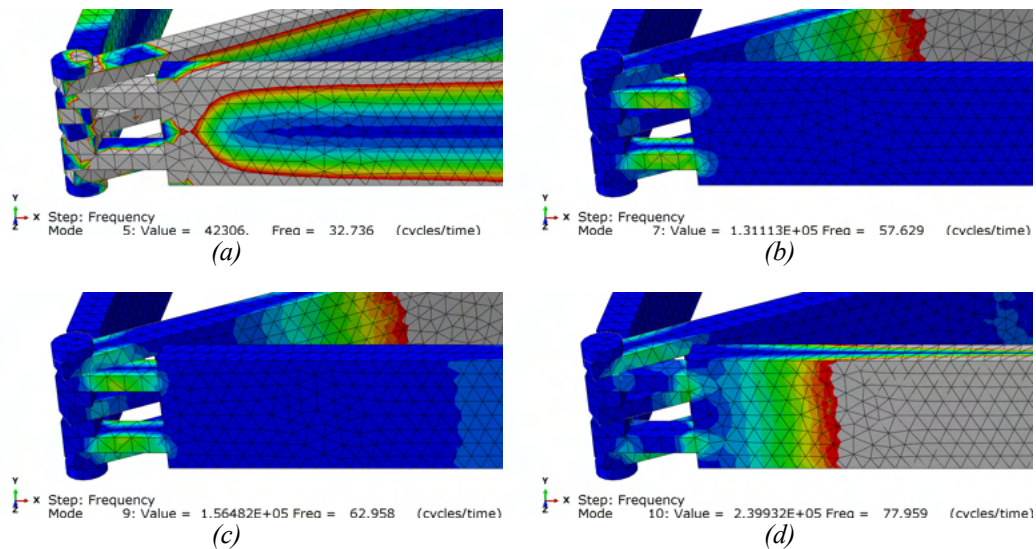


Fig. 4: Mode shapes of the (a) –(j) first to 10<sup>th</sup> modes of vibration of the metal frame structure obtained through FE analysis

After verifying the fidelity of the updated FE model, it was utilised to generate the high-resolution strain energy distributions in the metal frame structure in the different modes of vibration, so a proper mode could be selected for the vibrothermographic tests. Among the ten modes of vibration studied above, there were relatively high levels of strain energy in the regions of interest in four modes, namely modes 5, 7, 9 and 10. To present the results, the strain energy distributions in one of the joints in these four modes of vibration are shown in Fig. 5. In Fig. 5, an equal rainbow-based colour scale was applied to all plots to ensure consistency and allow more convenient comparison of the results.



*Fig. 5: Strain energy distributions in one of the joints in the (a) –(d) fifth, seventh, ninth and 10<sup>th</sup> modes of vibration of the metal frame structure obtained through FE analysis*

To optimise the selection, besides the strain energy in the joints, another major factor that must be considered was the difficulty for each mode to be excited effectively in the vibrothermographic tests. As an electrodynamic shaker was to be applied as the method of excitation, the location of excitation needed to have a greater local mode shape in the direction of excitation so that the targeted mode(s) can be excited energetically. Based on this criterion, among the four candidates listed above, the fifth mode was eliminated first as it was an out-of-plane mode. For modes 7 and 9, based on the mode shapes presented in Figs. 3 and 4, it would be preferable to attach the shaker to one of the cross-beams, which was impractical to achieve experimentally. For these reasons, the 10<sup>th</sup> mode of vibration was selected as the target mode in the vibrothermographic tests, where this mode would be pertinently excited to ensure sufficient strain energy and frictional heat generation in the joints.

### **Experimental Modal Testing with Different Bolt Load Levels**

With the completion of the initial modal analysis to generate the necessary information on the parameters of excitation, vibrothermographic testing of the metal frame structure could be started. In order to excite the 10<sup>th</sup> mode of vibration more effectively, the electrodynamic shaker was attached at a location with large deflection, as shown in Fig. 1.

As the objective of the vibrothermographic tests was to investigate the relationship between the frictional heat generation, modal damping and the condition of the joints, six different bolt load levels, namely 0 N m, 0.5 N m, 1.5 N m, 3.0 N m, 4.5 N m and 6.0 N m, were selected and applied, with each of which a separate modal analysis and a vibrothermographic test would be performed to measure the modal damping and the frictional heating. In all six cases, the bolt



loads were applied precisely using a digital torque wrench. Because only one joint was to be inspected, the bolt loads were only applied to the bolt in the inspected joint while the bolt loads in the other three joints were maintained at zero.

As mentioned above, with each bolt load level, an individual modal analysis was conducted, the goal of which was to extract the relevant modal parameters while ensuring that the bolt load was applied successfully and the changes in the natural frequency would not cause considerable differences to the subsequent vibrothermographic tests. During the six modal tests, the parameters on the signal generator and the power amplifier remained unchanged, so a voltage of 4 V was supplied to the shaker in each case. After the completion of the six tests, the natural frequencies and the damping ratios of the 10<sup>th</sup> mode of vibration were calculated from the drive-point frequency response functions using the half-power point method [45]. Setting the natural frequency when the load was 6.0 N m as the reference, the frequency differences when the bolt load was changed to the other five values were calculated. The results are summarised below in Table 3. As a demonstration, the measured frequency response function with 0 N m bolt loads in all joints is displayed in Fig. 6.

Table 3: Natural frequencies and damping ratios of the 10<sup>th</sup> mode of vibration at different bolt load levels

Bolt Load (N m)	0	0.5	1.5	3.0	4.5	6.0
Frequency (Hz)	75.44	75.97	76.32	76.79	77.15	77.56
Freq. Change (%)	-2.73	-2.05	-1.60	-0.99	-0.53	0
Damping Ratio (%)	1.22	1.55	2.70	2.10	1.73	1.78

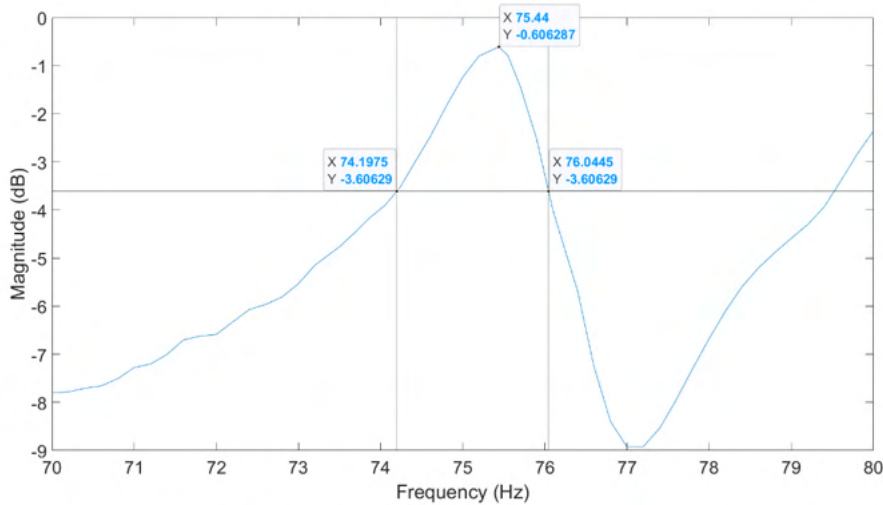


Fig. 6: The drive-point frequency response function around the 10<sup>th</sup> mode when the bolt loads in the joints were 0 N m

As demonstrated in Table 3, as the bolt load decreased, the natural frequency of the 10<sup>th</sup> mode of vibration was reduced monotonically, which should be attributed to the changes in stiffness. This phenomenon indicated that the bolt load was successfully applied, and the changes were not significant enough to cause considerable differences in the subsequent tests. However, a non-monotonic relationship was observed between the damping ratio and the bolt load. This relationship would be explained later with the results from the vibrothermographic tests.

## Experimental Vibrothermographic Testing

As the modal tests using these six different bolt loads had been completed, which yielded the observations above, the vibrothermographic tests targeting the 10<sup>th</sup> mode of vibration could be performed with the same six bolt load levels. In each of these six tests, a harmonic excitation force with frequency matching the natural frequency of the 10<sup>th</sup> mode was applied. The amplitudes of the excitation forces were kept approximately identical and unchanged from the modal tests by using the same input voltage of 4 V. For completeness, although it was possible to attach a force gauge on the drive rod between the electrodynamic shaker and the metal frame structure to measure the force directly, this plan was abandoned as it would introduce additional components and interfaces between the shaker and the excited structure, which was likely to lower the efficiency of the excitation while adding unnecessary constraints and uncertainties.

For data acquisition, a Nippon Avionics TH9100MR infrared camera, which has a resolution of  $320 \times 240$  and a maximum thermal sensitivity of  $< 0.02 \text{ }^\circ\text{C}$ , was utilised to measure the temperature changes during the tests. In all six tests, temperature data were recorded at 10 s intervals. Each of the tests lasted for 17 minutes, so 103 frames of data would be recorded. The timeline of events in the vibrothermographic tests is summarised in Table 4, which was strictly followed in all six tests. Because of the identical parameters applied and the same time points at which the data were captured, the data acquired in the six tests could be compared on the same basis.

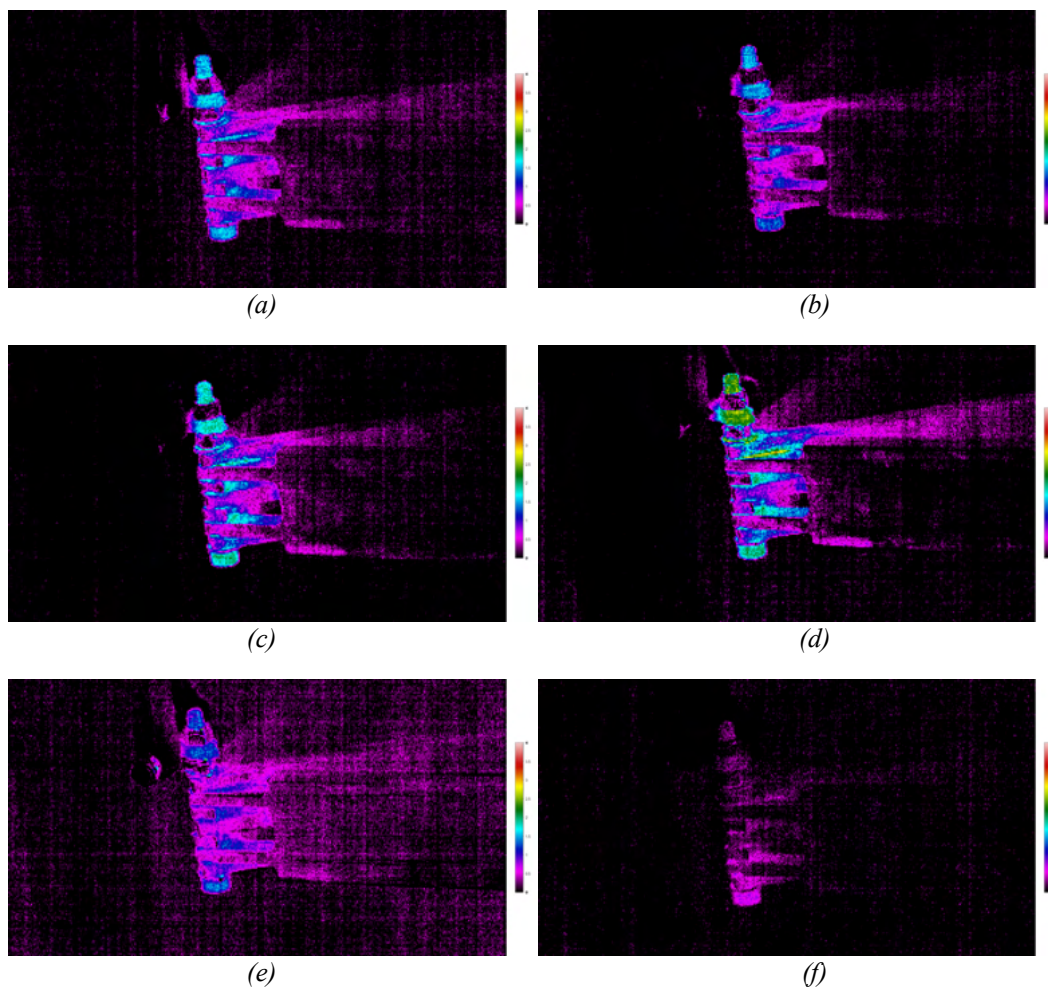


*Fig. 7: Infrared images taken at 7:00 of the vibrothermographic tests sorted in descending order by the bolt load ((a) - (f) 6.0 N m , 4.5 N m, 3.0 N m, 1.5 N m, 0.5 N m and 0 N m)*

*Table 4: Timeline of events in the vibrothermographic tests*

Time (min:s)	Event
0:00	Data recording started
2:00	Electrodynamic shaker turned on
7:00	Infrared images displayed in Fig. 7 taken
12:00	Electrodynamic shaker turned off Infrared images displayed in Fig. 8 taken
17:00	Data recording stopped

As described in Table 4, data recording had been started before the shaker was turned on, so the initial temperature data could be captured. The initial temperature data were then subtracted from the subsequent frames to reveal the net temperature changes. After the electrodynamic shaker was turned off, the measurement continued for another five minutes in order to capture the heat dissipation process to ensure that there would not be any unexpected behaviours during the tests. Among the 103 frames recorded in each test, two images were extracted and are presented here as examples. These example images, which are shown in Figs 7 and 8, were taken at five minutes and 10 minutes respectively after the shaker was turned on.

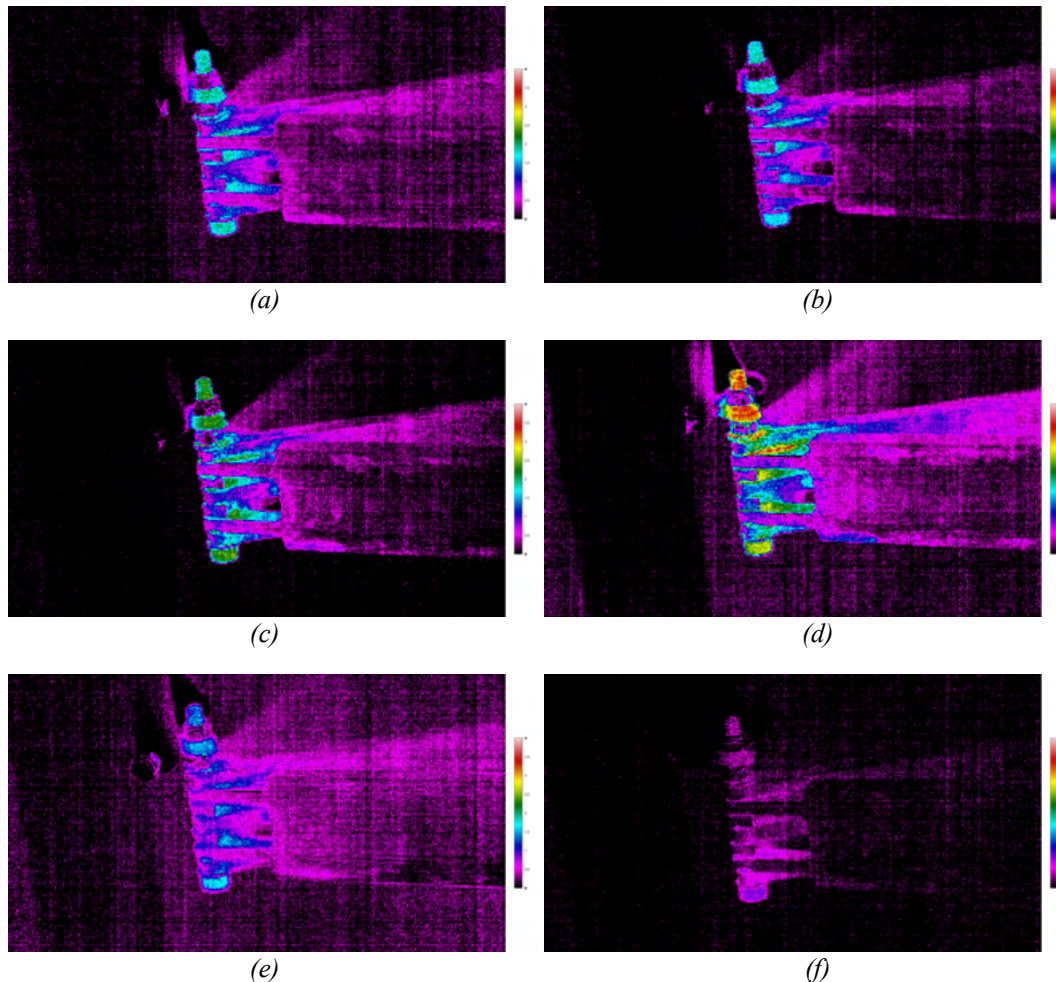


*Fig. 8: Infrared images taken at 12:00 of the vibrothermographic tests sorted in descending order by the bolt load ((a)-(f) 6.0 N m , 4.5 N m, 3.0 N m, 1.5 N m, 0.5 N m and 0 N m)*

Based on the results in Figs 7 and 8, where an equal temperature scale spanning from 0 to 4 °C was used for all the images, it was first demonstrated that the friction between the contact surfaces in the joint was able to generate clearly detectable temperature increases. The frictional



heat generation was significantly more rapid than the heat dissipation, so highly localized hot spots were developed. For all bolt load levels except the zero-load case, multiple hot spots with maximum temperature increases greater than 0.5 °C became observable within two minutes after the shaker was turned on, showing the efficiency of this vibrothermographic approach. These observations have successfully verified the viability of the vibrothermographic method in terms of revealing the structural degradation in the metal frame structure caused by the decreased bolt tightness levels with the distinct advantage of short measurement time.

To analyse the data quantitatively, temperature increases were extracted from the topmost interface in the joint, which was achieved by creating a rectangular measurement box surrounding this region as shown in Fig. 9. The maximum temperature increases in this interface after the excitation was started for five and 10 minutes, which corresponded to the images shown in Figs 7 and 8, were extracted and plotted as displayed in Fig. 10.

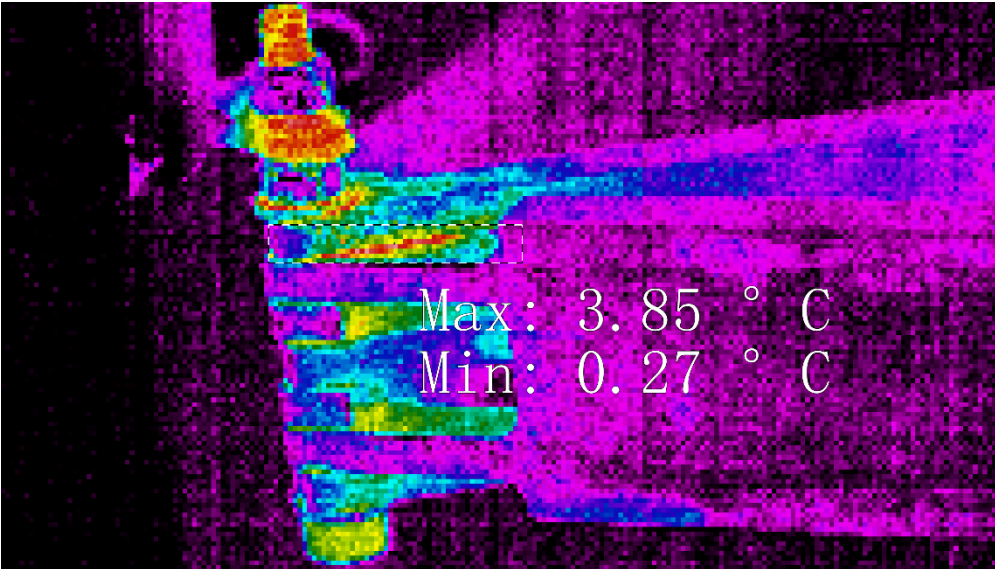


Fig. 9: The rectangular box created around the topmost interface to extract the temperature increases

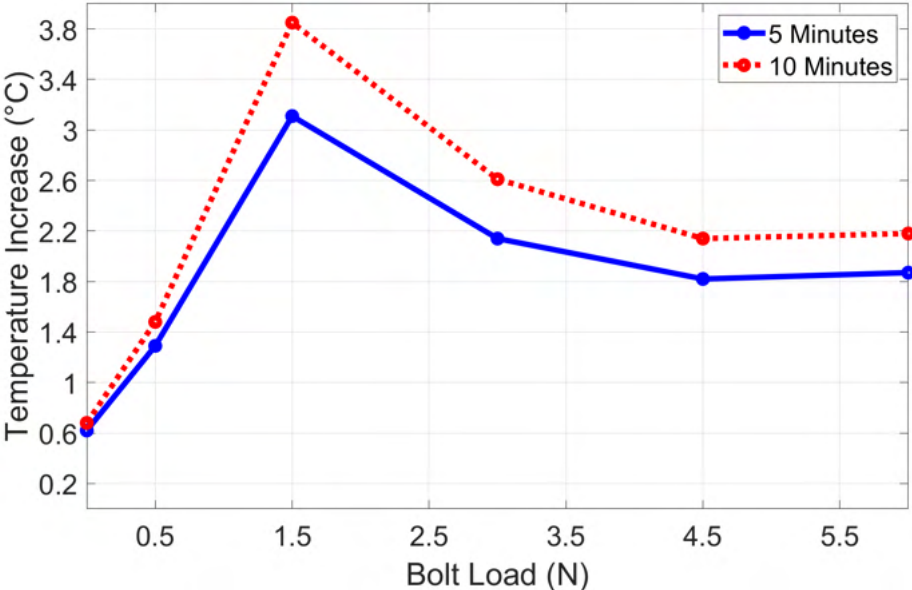
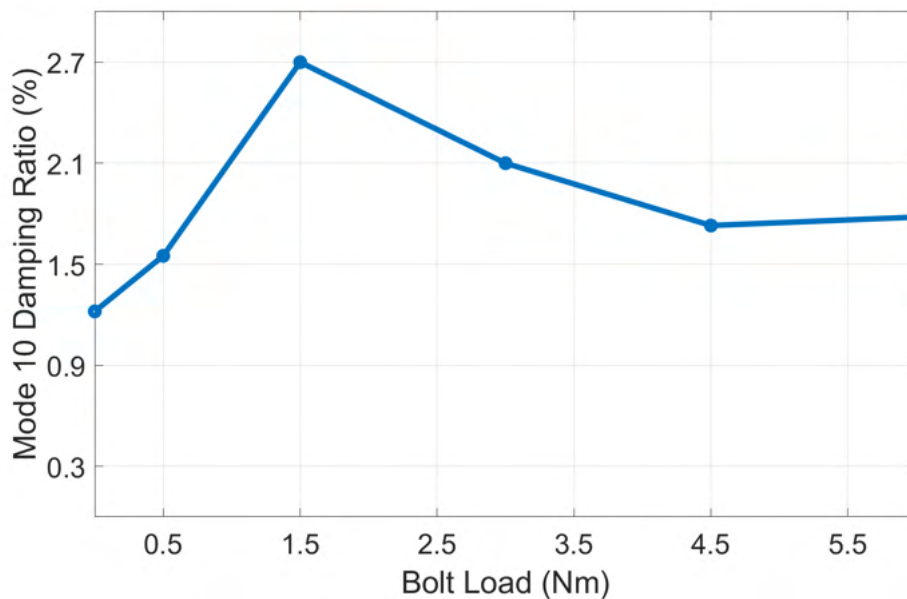


Fig. 10: Maximum temperature increase (°C) in the topmost interface recorded at five and 10 minutes after the electrodynamic shaker was turned on

By inspecting the images in Figs. 7 and 8 and the plot in Fig. 10, it could be observed that, for the temperature data recorded at the same times across the six tests with identical set-up and unchanged parameters, as the bolt load decreased, the frictional heat generation rate represented by the temperature values firstly increased, until a maximum was reached, and then started to decrease rapidly.

In addition, the trend of the temperature increases shown in Fig. 10 also matched the changes in the damping due to the different bolt load levels, which have been summarised in Table 3. To demonstrate this relationship more clearly, the damping ratios of the 10<sup>th</sup> mode at the different bolt load levels were also plotted as shown in Fig. 11.



*Fig. 11: Damping ratios of the 10<sup>th</sup> mode of vibration at different bolt load levels*

By comparing the plots in Figs. 10 and 11, both the temperature increases and the damping ratio followed a bell-curve-shaped relationship with the bolt load. This phenomenon was comprehensible, demonstrating that the primary source of energy dissipation in the system was the frictional heating in the joints. This finding verified the possibility of utilising non-contact thermal measurements as the representations of the changes in damping, which would be especially useful in applications where the latter could be difficult to measure.

In addition, it was observed that as the bolt load decreased, the natural frequencies of the structure also decreased monotonically due to the reduction in stiffness. For this reason, the measured temperature data may also be utilised as estimators of the changes in the natural frequencies.

Based on the results from the vibrothermographic tests, it was demonstrated that as the integrity of the structure worsened, the frictional heat generation rate firstly increased then decreased as the failure, which was simulated by the zero bolt load, approached, under the conditions that the amplitude and frequency of vibration remained approximately unchanged.

## Conclusion

In this research, a modal-based vibrothermographic approach was studied. It was demonstrated that this method could be utilised to detect the structural degradation simulated by the different bolt load levels. To summarise, as the bolt load decreased, which represented the loss of tightness in the joint, the frictional heat generation rate would first increase, and decrease rapidly as failure approached.

In addition to the significance in detecting issues and monitoring the health conditions directly, this vibrothermographic method could also be used to reveal the changes in certain dynamic properties. Due to the relationship between energy dissipation and frictional heating, the temperature data measured in a non-contact manner could be employed to estimate the changes in damping of the structure.

Besides the outcomes from this research summarised above, this vibrothermographic approach could be further developed for improved general applicability.

Firstly, in the planning phase in this research, the strain energy distribution was obtained through FE analyses on an updated model due to the limitations on the actual number of sensors that may be placed on the physical structure, which would restrict the resolution of the results measured experimentally. However, should the experimental infrastructure be available, full-field strain measurements—rather than sparse strain gauge measurements—performed directly on the physical structure could be particularly useful for providing more precise information on the dynamic behaviours of the structure.

Secondly, the structural degradation in this research was simulated by the changed bolt loads in the joints. It would be beneficial to apply this method in a wider range of applications to verify that this vibrothermographic method could still be applied for detecting the changed dynamic properties and health conditions of the structures.

Finally, because of the configuration of the metal frame structure, frictional heat generation was the dominant source of energy dissipation during the induced vibrations. Replicating this procedure in applications under different scenarios would improve the robustness of the vibrothermographic approach in terms of revealing the dynamic changes in the structure.

## References

1. C. Devriendt, F. Magalhães, W. Weijtjens, G. De Sitter, Á. Cunha, and P. Guillaume, “Structural health monitoring of offshore wind turbines using automated operational modal analysis,” *Structural Health Monitoring*, vol. 13, no. 6, pp. 644–659, Nov. 2014.
2. A. J. Dammika, K. Kawarai, H. Yamaguchi, Y. Matsumoto, and T. Yoshioka, “Analytical Damping Evaluation Complementary to Experimental Structural Health Monitoring of Bridges,” *Journal of Bridge Engineering*, vol. 20, no. 7, p. 4014095, Jul. 2015.
3. P. Asadollahi and J. Li, “Statistical Analysis of Modal Properties of a Cable-Stayed Bridge through Long-Term Wireless Structural Health Monitoring,” *Journal of Bridge Engineering*, vol. 22, no. 9, p. 4017051, Sep. 2017.



4. D. Montalvão, D. Karanatsis, A. M. Ribeiro, J. Arina, and R. Baxter, “An experimental study on the evolution of modal damping with damage in carbon fiber laminates,” *Journal of Composite Materials*, vol. 49, no. 19, pp. 2403–2413, Aug. 2015.
5. G. Kawiecki, “Modal damping measurement for damage detection,” *Smart Materials and Structures*, vol. 10, no. 3, pp. 466–471, Jun. 2001.
6. E. G. Henneke and T. S. Jones, “Detection of Damage in Composite Materials by Vibrothermography,” *Nondestructive Evaluation and Flaw Criticality for Composite Materials*, Dec. 1979.
7. E. G. Henneke, K. L. Reifsnider, and W. W. Stinchcomb, “Thermography — An NDI Method for Damage Detection,” *JOM*, vol. 31, no. 9, pp. 11–15, Sep. 1979.
8. W. W. Stinchcomb, *Mechanics of Nondestructive Testing*. Springer US, 1980.
9. E. G. Henneke, K. L. Reifsnider, and W. W. Stinchcomb, “Vibrothermography: Investigation, Development, and Application of a New Nondestructive Evaluation Technique,” Engineering Science and Mechanics Department, Virginia Polytechnic Institute and State University Blacksburg, VA 24061, 1986.
10. T. Stepinski, T. Uhl, and W. Staszewski, *Advanced Structural Damage Detection: From Theory to Engineering Applications*. Wiley, 2013.
11. X. Chi, D. Di Maio, and N. Lieven, “Dynamic response and energy loss in jointed structures using finite element methods: application to an aero-engine casing assembly,” in *Proceedings of International Conference on Noise and Vibration Engineering, ISMA2018 and International Conference on Uncertainty in Structural Dynamics, USD2018*, 2018, pp. 1835–1849.
12. X. Chi, D. Di Maio, and N. A. J. Lieven, “Health monitoring of bolted joints using modal-based vibrothermography,” *SN Applied Sciences*, vol. 2, no. 8, Jul. 2020.
13. R. A. Ibrahim and C. L. Pettit, “Uncertainties and dynamic problems of bolted joints and other fasteners,” *Journal of Sound and Vibration*, vol. 279, no. 3, pp. 857–936, Jan. 2005.
14. L. Gaul and J. Lenz, “Nonlinear dynamics of structures assembled by bolted joints,” *Acta Mechanica*, vol. 125, no. 1, pp. 169–181, Mar. 1997.
15. C. W. Schwingshackl, D. Di Maio, I. Sever, and J. S. Green, “Modeling and Validation of the Nonlinear Dynamic Behavior of Bolted Flange Joints,” *Journal of Engineering for Gas Turbines and Power*, vol. 135, no. 12, Sep. 2013.
16. C. J. Hartwigsen, Y. Song, D. M. McFarland, L. A. Bergman, and A. F. Vakakis, “Experimental study of non-linear effects in a typical shear lap joint configuration,” *Journal of Sound and Vibration*, vol. 277, no. 1, pp. 327–351, Oct. 2004.
17. X. Ma, L. Bergman, and A. Vakakis, “IDENTIFICATION OF BOLTED JOINTS THROUGH LASER VIBROMETRY,” *Journal of Sound and Vibration*, vol. 246, no. 3, pp. 441–460, Sep. 2001.

18. D. Di Maio, "Identification of Dynamic Nonlinearities of Bolted Structures Using Strain Analysis," in *Nonlinear Dynamics, Volume 1*, Cham, 2016, pp. 387–414.
19. D. Di Maio, A. Bozzo, and N. Peyret, "Response phase mapping of nonlinear joint dynamics using continuous scanning LDV measurement method," *AIP Conference Proceedings*, vol. 1740, no. 1, p. 70003, Jun. 2016.
20. J. Renshaw, J. C. Chen, S. D. Holland, and R. Bruce Thompson, "The sources of heat generation in vibrothermography," *NDT & E International*, vol. 44, no. 8, pp. 736–739, Dec. 2011.
21. R. B. Mignogna, R. E. Green, J. C. Duke, E. G. H. II, and K. L. Reifsnider, "Thermographic investigation of high-power ultrasonic heating in materials," *Ultrasonics*, vol. 19, no. 4, pp. 159–163, 1981.
22. C. J. Pye and R. D. Adams, "Heat emission from damaged composite materials and its use in nondestructive testing," *Journal of Physics D: Applied Physics*, vol. 14, no. 5, pp. 927–941, 1981.
23. C. J. Pye and R. D. Adams, "Detection of damage in fibre reinforced plastics using thermal fields generated during resonant vibration," *NDT International*, vol. 14, no. 3, pp. 111–118, 1981.
24. M. Morbidini, P. Cawley, T. J. Barden, D. P. Almond, and P. Duffour, "A New Approach for the Prediction of the Thermosonic Signal from Vibration Records," *AIP Conference Proceedings*, vol. 820, no. 1, pp. 558–565, 2006.
25. M. Morbidini, P. Cawley, T. Barden, D. Almond, and P. Duffour, "Prediction of the thermosonic signal from fatigue cracks in metals using vibration damping measurements," *Journal of Applied Physics*, vol. 100, no. 10, p. 104905, 2006.
26. B. Kang and P. Cawley, "Low Power PZT Exciter for Thermosonics," *AIP Conference Proceedings*, vol. 894, no. 1, pp. 484–491, 2007.
27. B. Kang and P. Cawley, "MULTI-MODE EXCITATION SYSTEM FOR THERMOSONIC TESTING OF TURBINE BLADES," *AIP Conference Proceedings*, vol. 975, no. 1, pp. 520–527, 2008.
28. B. Kang, H. Lee, and C. Lee, "Performance of a small PZT exciter for thermosonic non-destructive testing," in *INTELEC 2009 – 31st International Telecommunications Energy Conference*, Incheon, South Korea, 2009, pp. 1–4.
29. S. D. Holland, C. Uhl, and J. Renshaw, "VIBROTHERMOGRAPHIC CRACK HEATING: A FUNCTION OF VIBRATION AND CRACK SIZE," *AIP Conference Proceedings*, vol. 1096, no. 1, pp. 489–494, 2009.
30. S. D. Holland et al., "Quantifying the vibrothermographic effect," *NDT & E International*, vol. 44, no. 8, pp. 775–782, 2011.

31. I. Solodov, M. Rahammer, D. Derusova, and G. Busse, “Highly-efficient and noncontact vibro-thermography via local defect resonance,” *Quantitative InfraRed Thermography Journal*, vol. 12, no. 1, pp. 98–111, 2015.
32. G. Bai, B. Lamboul, J.-M. Roche, and S. Baste, “Investigation of multiple cracking in glass/epoxy 2D woven composites by vibrothermography,” *Quantitative InfraRed Thermography Journal*, vol. 13, no. 1, pp. 35–49, 2016.
33. N. Harwood and W. M. Cummings, *Thermoelastic Stress Analysis*. CRC Press, 1991.
34. J. Rantala, D. Wu, and G. Busse, “Amplitude-modulated lock-in vibrothermography for NDE of polymers and composites,” *Research in Nondestructive Evaluation*, vol. 7, no. 4, pp. 215–228, 1996.
35. J.-C. Krapez, F. Taillade, and D. Balageas, “Ultrasound-lockin-thermography NDE of composite plates with low power actuators. Experimental investigation of the influence of the Lamb wave frequency,” *Quantitative InfraRed Thermography Journal*, vol. 2, no. 2, pp. 191–206, 2005.
36. I. Solodov, M. Rahammer, D. Derusova, and G. Busse, “Highly-efficient and noncontact vibro-thermography via local defect resonance,” *Quantitative InfraRed Thermography Journal*, vol. 12, no. 1, pp. 98–111, 2015.
37. R. Montanini and F. Freni, “Correlation between vibrational mode shapes and viscoelastic heat generation in vibrothermography,” *NDT & E International*, vol. 58, pp. 43–48, Sep. 2013.
38. J. Renshaw, S. D. Holland, and D. J. Barnard, “Viscous material-filled synthetic defects for vibrothermography,” *NDT & E International*, vol. 42, no. 8, pp. 753–756, 2009.
39. X. Chi, D. D. Maio, and N. A. J. Lieven, “Modal-based vibrothermography using feature extraction with application to composite materials,” *Structural Health Monitoring*, vol. 19, no. 4, pp. 967–986, 2020.
40. J. H. Dieterich, “Time-dependent friction and the mechanics of stick-slip,” *Pure and Applied Geophysics*, vol. 116, no. 4, pp. 790–806, 1978.
41. J. Woodhouse, T. Putelat, and A. McKay, “Are there reliable constitutive laws for dynamic friction?,” *Philosophical Transactions of the Royal Society A: Mathematical, Physical and Engineering Sciences*, vol. 373, no. 2051, p. 20140401, 2015.
42. R. I. Leine, D. H. van Campen, A. de Kraker, and L. van den Steen, “Stick-Slip Vibrations Induced by Alternate Friction Models,” *Nonlinear Dynamics*, vol. 16, pp. 41–54, May 1998.
43. K. Popp and P. Stelzer, “Stick-slip vibrations and chaos,” *Philosophical Transactions of the Royal Society of London. Series A: Physical and Engineering Sciences*, vol. 332, no. 1624, pp. 89–105, 1990.
44. J. L. du Bois, “Adaptive Fuselage Response Suppression,” University of Bristol, 2009.

45. D. J. Ewins, *Modal Testing: Theory, Practice and Application*, 2nd ed. Research Studies Press LTD, 2000.